Inorganic Chemistry

Communication

pubs.acs.org/IC

# New Method for Exploring Deactivation Kinetics in Copper-Catalyzed Atom-Transfer-Radical Reactions

Timothy J. Zerk and Paul V. Bernhardt*

School of Chemistry and Molecular Biosciences, University of Queensland, Brisbane 4072, Australia

Supporting Information

**ABSTRACT:** Copper polyamine complexes are among the most utilized catalysts for controlled radical polymerization reactions. Copper(I) complexes may react reversibly with an alkyl halide to form an alkyl radical, which promotes polymerization, and a copper(II) halido complex in a step known as activation. The kinetics of the reverse reaction between the alkyl radical and higher oxidation-state copper complex (deactivation) are less studied because these reactions approach diffusion-controlled rates, and it is difficult to isolate or quantify the concentration of the alkyl radical ($R^{\bullet}$) in situ. Herein we report a broadly applicable electrochemical technique for simultaneously measuring the kinetics of deactivation and kinetics of activation.

Atom-transfer-radical polymerization (ATRP) is one of the most important forms of controlled reversible-deactivation radical polymerization.[1−4] In ATRP, a transition-metal complex, typically copper(I), reacts with an alkyl halide initiator (R−X) to form an alkyl radical ($R^{\bullet}$) and a halidocopper(II) complex ($k_{act}$ in Scheme 1). The free radical either reacts with a monomer,

**Scheme 1. Copper-Catalyzed ATRP Equilibrium**[a]

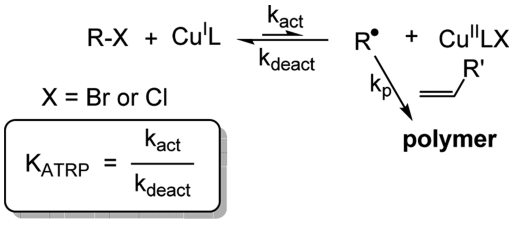


[a] L = multidentate ligand. R−X is the alkyl halide initiator.

initiating polymerization ($k_p$), or recombines reversibly with the halidocopper(II) complex to regenerate the reactants and deactivate the radical ($k_{deact}$ in Scheme 1). ATRP utilizes the dynamic equilibrium between these two oxidation states of the catalyst, which is biased heavily in the direction of the dormant initiator R−X [and copper(I)] to suppress the concentration of the free radical ($R^{\bullet}$), thus avoiding undesirable radical−radical coupling (termination). This leads to excellent molecular weight control and dispersity for the resulting polymer products.[4−6] The ability to determine the rates of both the forward and reverse reactions in the ATRP equilibrium ($k_{act}/k_{deact} = K_{ATRP}$) is important for understanding mechanistic details and for determining the appropriate catalyst−solvent−initiator combinations for a given monomer. Various techniques[7−10] have been applied to measure the reaction rates for systems with activation rates as high as $10^4$ $M^{-1}$ $s^{-1}$. We recently reported[11] a methodology especially suited to even more active catalysts using cyclic voltammetry (CV) to monitor the homogeneous activation reaction. Enhancement of the cathodic current in the presence of an alkyl halide initiator provides a direct measure of the overall activation/deactivation reaction.

The accurate measurement of $k_{deact}$ is more difficult because the bimolecular reaction approaches diffusion-controlled limits ($\sim 10^7-10^8$ $M^{-1}$ $s^{-1}$) and the radical $R^{\bullet}$ is unable to be isolated or its concentration quantified in situ because it reacts with itself, and this limits the experimental methodology for determining $k_{deact}$.[12−15] One technique for probing $k_{deact}$ utilizes radical clock-reactions. Typically, $R^{\bullet}$ is generated in the presence of the nitroxide radical trap 2,2,6,6-(tetramethylpiperidin-1-yl)oxyl (TEMPO) and deactivator $Cu^{II}LX$.[9] The two competing products, R−TEMPO and R−X, are quantified, and the relative amount of each provides $k_{deact}$ based upon the known TEMPO + $R^{\bullet}$ rate constant, which is both solvent-dependent and dependent on the structure of $R^{\bullet}$. This is a serious limitation because kinetic data for each TEMPO + $R^{\bullet}$ system (in each solvent) must be determined. A direct method utilizes time-resolved electron paramagnetic reosnance to measure the rate of disappearance of radicals in the presence of a deactivating copper(II) complex.[12]

Herein we report a technique for determining $k_{deact}$, which (i) does not rely on any previously determined rate constants, (ii) simultaneously leads to the corresponding value of $k_{act}$ for the system, and (iii) is broadly applicable for determining the kinetics of both of these reactions across a variety of solvent−catalyst−initiator combinations including highly reactive systems. A key feature of our electrochemical approach for studying the kinetics of atom-transfer-radical activation/deactivation reactions is that it utilizes a resting solution of $Cu^{II}LX$ (X = Br, a stable and well-defined complex of known concentration), which is reduced anaerobically (at potential $E_{Br}$) to produce the active form of the catalyst $Cu^{I}L$ (Scheme 1) in situ. Electrochemical simulations, which include all bimolecular rate constants for the coupled chemical reactions, e.g., $k_{cat}$ and $k_{deact}$, reproduce the experimental cyclic voltammograms across a range of RBr concentrations and scan rates by optimizing the unknown rate constants in the mechanism.[11,16]

The precatalyst in this work is the complex $[Cu^{II}(PMDETA)Br]^+$ (PMDETA = *N*,*N*,*N*′,*N*″,*N*″-pentamethyldiethylenetri-

**Received:** September 11, 2014
**Published:** October 13, 2014

   dx.doi.org/10.1021/ic5022005 | *Inorg. Chem.* 2014, 53, 11351−11353

amine = L).[17−19] The solvent is dry dimethyl sulfoxide (DMSO; with a 0.1 M $Et_4N{\cdot}ClO_4$ supporting electrolyte), and three different alkyl bromide (RBr) initiators are employed: ethyl α-bromoisobutyrate (EBriB), methyl 2-bromopropanoate (MBP), and benzyl bromide (BnBr).

Historically, $k_{deact}$ has been assumed to be relatively constant, while $k_{act}$ varies over several orders of magnitude ($10^{-4}$−$10^3$ $M^{-1}$ $s^{-1}$) for a given ligand−solvent system.[14] It is important to emphasize that the number of accurately (independently) determined values of $k_{deact}$ in the literature is far outweighed by the corresponding $k_{act}$ values. Furthermore, the majority of published $k_{deact}$ values have been calculated as opposed to directly measured.[14] Here we illustrate that the kinetics of the deactivation reaction can be determined independently. The radical scavenger TEMPO is employed to ensure that the reaction shown in Scheme 2 becomes unidirectional; i.e., deactivation is prevented by the rapid removal of $R^{\bullet}$ from the system. Figure 1 illustrates this methodology. First the CV in broken lines (in the absence of EBriB) is simply due to the reversible one-electron $[Cu(PMDETA)Br]^{+/0}$ response (E mechanism). The addition of 3 equiv of EBriB enhances the catalytic current, and the CV begins to change to a more sigmoidal form. This is a result of the coupled (catalytic) chemical reaction ($[Cu^{I}(PMDETA)]^+$ + EBriB), which regenerates $[Cu^{II}(PMDETA)Br]^+$ at low potential and is immediately reduced again at the electrode ($EC_{cat}$ mechanism). The addition of TEMPO leads to *further enhancement* of the current (maximized upon the addition of 2 equiv of TEMPO) because none of $[Cu^{II}(PMDETA)Br]^+$ regenerated at the electrode surface by the activation reaction is lost through the reverse deactivation reaction (Scheme 2). Similar experiments were performed for each of the initiators EBriB, MBP, and BnBr (see Figure S1 in the Supporting Information, SI).

**Scheme 2. Mechanism for Electrochemically Stimulated Atom Transfer Starting with $[Cu^{II}LBr]^+$**

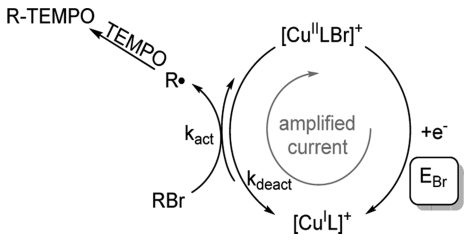


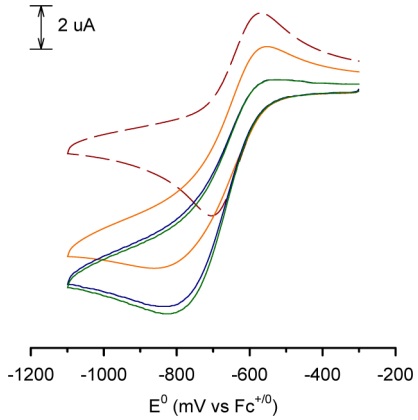


**Figure 1.** CV of 1 mM $[Cu^{II}(PMDETA)Br]Br$ in DMSO (0.1 M $Et_4N{\cdot}ClO_4$) without EBriB (dashed curve) in the presence of 3 mM EBriB (yellow) and successive amounts of TEMPO (2 mM TEMPO, blue; 5 mM TEMPO, green). Sweep rate 50 mV $s^{-1}$.

The voltammetry of $[Cu^{II}(PMDETA)Br]^+$ in the presence of a sufficient concentration of TEMPO to make the otherwise reversible activation reaction unidirectional was investigated at various concentrations of each initiator and at different sweep rates. The voltammetry was then simulated to match the experimental data according to the mechanism in Scheme 2. The only parameter that was allowed to vary during the simulation was $k_{act}$. The remaining parameters in the simulation (diffusion coefficients and heterogeneous electron-transfer rates) were determined by simulating the voltammetry in the absence of an initiator as described.[11,16] Figure 2 compares the experimental and simulated voltammograms. The excellent match between the experiment and simulation and the sensitivity of the simulation to $k_{act}$ gives us confidence in the accuracy of this number. It can be seen that the catalytic current is enhanced and the anodic peak gradually disappears with increasing initiator concentration. The value for $k_{deact}$ in the mechanism was irrelevant under these conditions because deactivation is quenched; i.e., even values at the diffusion limit ($10^9$−$10^{10}$ $M^{-1}$ $s^{-1}$) had no effect on the simulation.

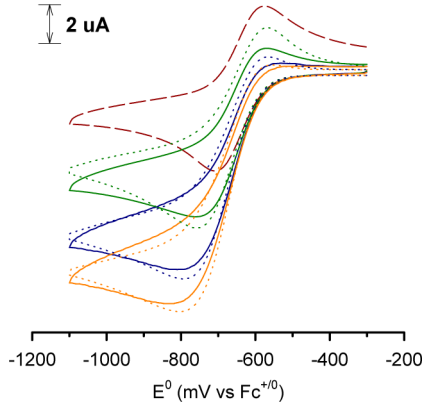


**Figure 2.** Experimental (solid lines) and simulated (dotted lines) cyclic voltammograms of 1 mM $[Cu^{II}(PMDETA)Br]Br$ in DMSO (0.1 M $Et_4N{\cdot}ClO_4$) with excess TEMPO (15 mM): red dashed curve, no EBriB; green curves, 1 mM EBriB; blue curves, 3 mM EBriB; yellow curves, 5 mM EBriB. Sweep rate 50 mV $s^{-1}$.

The resulting values for $k_{act}$ are shown in Table 1, which vary across ∼2 orders of magnitude in the expected order EBriB (tertiary bromide) > MBP (secondary bromide) > BnBr (primary bromide). This trend has been reported independently for $[Cu^{I}(PMDETA)Br]$ in MeCN using a different methodology.[20]

**Table 1. $k_{act}$ and $k_{deact}$ Values Determined from This Work (∼10% Uncertainty)**

| | EBriB | MBP | BnBr |
|---|---|---|---|
| $k_{act}$ ($M^{-1}$ $s^{-1}$) | $2.4 \times 10^3$ | $2.5 \times 10^2$ | $4.5 \times 10^1$ |
| $k_{deact}$ ($M^{-1}$ $s^{-1}$) | $1.8 \times 10^6$ | $7.6 \times 10^6$ | $8.6 \times 10^5$ |
| $K_{ATRP}$ | $1.3 \times 10^{-3}$ | $3.3 \times 10^{-5}$ | $5.2 \times 10^{-5}$ |

Having determined accurate and reliable values for $k_{act}$, the deactivation reaction was allowed to play a role in attenuating the catalytic cathodic current by performing the same experiments *in the absence* of TEMPO. As shown in Figure 1, the catalytic


dx.doi.org/10.1021/ic5022005 | *Inorg. Chem.* 2014, 53, 11351−11353

current is diminished in the absence of TEMPO because some of the alkyl radicals react with $Cu^{II}LBr$ at the electrode surface while some also react with each other to form R−R (see Figure S11 in the SI). Identical concentrations of the initiator and sweep rates were employed. Therefore, the differences between the catalytic currents in the absence and presence of TEMPO reflect the presence or absence of deactivation, respectively. The only parameter allowed to vary during the fitting process for these experiments was $k_{deact}$. A comparison between the experimental and simulated voltammograms in the absence of TEMPO is shown in Figure 3 for EBriB (see the SI for other examples

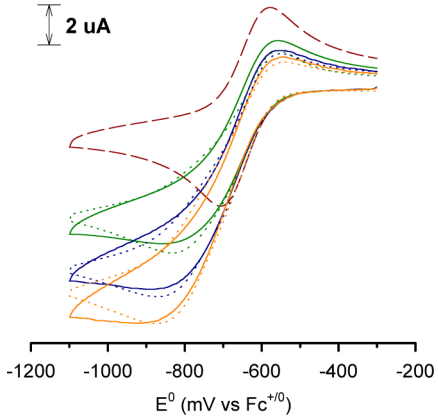


**Figure 3.** Experimental (solid lines) and simulated (dotted lines) CVs for 1 mM $[Cu^{II}(PMDETA)Br]Br$ in DMSO (0.1 M $Et_4N{\cdot}ClO_4$) in the absence of TEMPO: red dashed curve, no EBriB; green curves, 1 mM EBriB; blue curves, 3 mM EBriB; yellow curves, 5 mM EBriB. Sweep rate 50 mV $s^{-1}$.

including Figures S12 and S13, which illustrate the sensitivity of the simulations to the values of $k_{act}$ and $k_{deact}$). The optimized values of $k_{deact}$ are given in Table 1. Activation is known to be faster in DMSO than in other common ATRP solvents such as MeCN.[21] As such, the values reported in Table 1, while retaining the same trend in magnitude as MeCN, are also ∼3 orders of magnitude larger.[20]

The deactivation rate constant is also strongly influenced by the solvent, which also determines the position of the $Cu^{II}L^{2+} + X^- \rightleftharpoons Cu^{II}LX^+$ association equilibrium (or halidophilicity). Previous work has demonstrated that DMSO lowers the halidophilicity, leading to the loss of control over deactivation.[22] Table 1 reports values for deactivation that affirm this observation, where $k_{deact}$ is ∼2 orders of magnitude *lower* than that in MeCN.[14]

Expansion of the current work to a greater range of initiator−solvent systems will facilitate a better understanding of this phenomenon. Furthermore, we also wish to apply this technique to experimentally determine how various mixtures of organic solvent and water may alter the kinetics of deactivation, activation, or both. Exploring this new approach toward understanding the aspects of ATRP is currently underway in our laboratory using the herein-reported versatile and rapid technique for measuring deactivation rate constants.

## ■ ASSOCIATED CONTENT

### Ⓢ Supporting Information

Simulation parameters, all experimental conditions, and simulated and experimental CV at various sweep rates and concentrations of the initiator. This material is available free of charge via the Internet at http://pubs.acs.org.

## ■ AUTHOR INFORMATION

### Corresponding Author

*E-mail: p.bernhardt@uq.edu.au.

### Notes

The authors declare no competing financial interest.

## ■ ACKNOWLEDGMENTS

We gratefully acknowledge financial support from the Australian Research Council.

## ■ REFERENCES

(1) Wang, J. S.; Matyjaszewski, K. *J. Am. Chem. Soc.* **1995**, *117*, 5614−5615.
(2) Jenkins, A.; Jones, R.; Moad, G. *Pure Appl. Chem.* **2010**, *82*, 483−491.
(3) Kato, M.; Kamigaito, M.; Sawamoto, M.; Higashimura, T. *Macromolecules* **1995**, *28*, 1721−1723.
(4) Hadasha, W.; Klumperman, B. *Polym. Int.* **2014**, *63*, 824−834.
(5) Wei, H.; Perrier, S.; Dehn, S.; Ravarian, R.; Dehghani, F. *Soft Matter* **2012**, *8*, 9526−9528.
(6) Braunecker, W. A.; Matyjaszewski, K. *Prog. Polym. Sci.* **2007**, *32*, 93−146.
(7) Wang, Y.; Kwak, Y.; Buback, J.; Buback, M.; Matyjaszewski, K. *ACS Macro Lett.* **2012**, *1*, 1367−1370.
(8) Matyjaszewski, K.; Göbelt, B.; Paik, H.-j.; Horwitz, C. P. *Macromolecules* **2001**, *34*, 430−440.
(9) Matyjaszewski, K.; Paik, H.-j.; Zhou, P.; Diamanti, S. J. *Macromolecules* **2001**, *34*, 5125−5131.
(10) Pintauer, T.; Braunecker, W. A.; Collange, E.; Poli, R.; Matyjaszewski, K. *Macromolecules* **2004**, *37*, 2679−2682.
(11) Bell, C. A.; Bernhardt, P. V.; Monteiro, M. J. *J. Am. Chem. Soc.* **2011**, *133*, 11944−11947.
(12) Soerensen, N.; Barth, J.; Buback, M.; Morick, J.; Schroeder, H.; Matyjaszewski, K. *Macromolecules* **2012**, *45*, 3797−3801.
(13) Chambard, G.; Klumperman, B.; German, A. L. *Macromolecules* **2002**, *35*, 3420−3425.
(14) Tang, W.; Kwak, Y.; Braunecker, W.; Tsarevsky, N. V.; Coote, M. L.; Matyjaszewski, K. *J. Am. Chem. Soc.* **2008**, *130*, 10702−10713.
(15) Buback, M.; Morick, J. *Macromol. Chem. Phys.* **2010**, *211*, 2154−2161.
(16) Zerk, T. J.; Bernhardt, P. V. *Dalton Trans.* **2013**, *42*, 11683−11694.
(17) Ghelfi, F.; Parsons, A. F. *J. Org. Chem.* **2000**, *65*, 6249−6253.
(18) Ghelfi, F.; Bellesia, F.; Forti, L.; Ghirardini, G.; Grandi, R.; Libertini, E.; Montemaggi, M. C.; Pagnoni, U. M.; Pinetti, A.; De Buyck, L.; Parsons, A. F. *Tetrahedron* **1999**, *55*, 5839−5852.
(19) Benedetti, M.; Forti, L.; Ghelfi, F.; Pagnoni, U. M.; Ronzoni, R. *Tetrahedron* **1997**, *53*, 14031−14042.
(20) Tang, W.; Matyjaszewski, K. *Macromolecules* **2007**, *40*, 1858−1863.
(21) Horn, M.; Matyjaszewski, K. *Macromolecules* **2013**, *46*, 3350−3357.
(22) Braunecker, W. A.; Tsarevsky, N. V.; Gennaro, A.; Matyjaszewski, K. *Macromolecules* **2009**, *42*, 6348−6360.